INSTITUTE OF PHYSICS PUBLISHING SUPERCONDUCTOR SCIENCE AND TECHNOLOGY

Supercond. Sci. Technol. **16** (2003) 695–698 PII: S0953-2048(03)59320-4

Hall probe imaging of local hysteresis inversion and negative remanent fields near the edge of a YBCO thin film

A Crisan[1,2], A Pross[1], R G Humphreys[3] and S Bending[1]

[1] Department of Physics, University of Bath, Claverton Down, Bath BA2 7AY, UK
[2] National Institute for Materials Physics, PO Box MG-7, Bucharest 76900, Romania
[3] QinetiQ, St. Andrews Road, Malvern, Worcestershire WR14 3PS, UK

Received 28 January 2003, in final form 21 March 2003
Published 24 April 2003
Online at stacks.iop.org/SUST/16/695

Abstract
We report vortex imaging and local magnetometry studies near the edge of a YBCO thin film using scanning Hall probe microscopy (SHPM). Our data show some unusual features, namely local hysteresis inversion and negative remanent fields, which are semi-quantitatively explained in terms of a theoretical model of flux penetration in an infinite-long thin superconducting strip.

1. Introduction

Investigations of the magnetic properties of high-temperature superconductors (HTS) have revealed the existence of striking new vortex phenomena due, in part, to their strong crystalline anisotropy, very short coherence lengths and the much larger thermal energies available at high temperatures. The most direct information regarding vortex structures and dynamics is obtained through local measurements of the magnetic field within or at the surface of a superconducting sample, using various techniques, such as Lorentz microscopy, magnetic force microscopy, Bitter decoration, scanning Hall probe microscopy (SHPM), magneto-optical imaging and scanning SQUID microscopy. A detailed comparison of these complementary methods [1] reveals the existence of a trade-off between minimum detectable fields (highest for SQUID microscopy) and spatial resolution (highest for Lorentz microscopy), while SHPM is a niche technique which provides a unique compromise between spatial resolution ($\geqslant$200 nm) and minimum detectable field $\sim$100 nTHz$^{-1/2}$ ($T < 100$ K), making it particularly well adapted for investigating vortices in superconductors.

In this paper, we use the SHPM to generate images of vortex bundles and perform local magnetometry near the edge of a YBCO thin film. Our local measurements reveal the rather counter-intuitive features of inverse magnetic hysteresis and negative remanent fields. These unusual results are explained semi-quantitatively by Brandt's theoretical model of flux penetration in an infinite-long strip in the perpendicular geometry.

2. Experimental apparatus and sample preparation

We have used a state-of-the-art SHPM, which is described in detail elsewhere [2]. The Hall probe is mounted on the piezoelectric scanner tube of a commercial low-temperature scanning tunnelling microscope (STM) where a microfabricated semiconductor chip replaces the usual STM sharp tip. The sensor is patterned in a GaAs/AlGaAs heterostructure two-dimensional electron gas and consists of a 0.85 μm Hall probe and an etched mesa coated with a thin layer of gold which acts as an integrated STM tip. The sample is tilted 2°–3° with respect to the Hall probe to ensure that the STM tip (situated at the corner of the chip, about 13 μm away from the Hall probe) is always the closest point to it and bought into tunnelling contact with a 'stick-slip' inertial approach mechanism. The microscope is placed in a cryostat containing a 77–300 K variable-temperature insert. The measurements presented here were performed at a constant temperature of 80 K. An external copper coil and a controllable current source generated a magnetic field perpendicular to the sample, up to about 32 Oe. The experiments were performed in a 'flying' mode whereby the STM tip is used to find the surface after which the sample is retracted a fixed distance ($\sim$0.5 μm) out of tunnelling contact in order to perform rapid magnetic imaging without STM feedback. For this particular sample, particles on the surface prevented us from getting into intimate contact with it, and we estimate that the scan height is $\sim$1 μm. As a consequence, we were not able to image discrete vortices, but only localized vortex bundles. At the same time, the Hall sensor itself is not small enough for high-resolution Hall

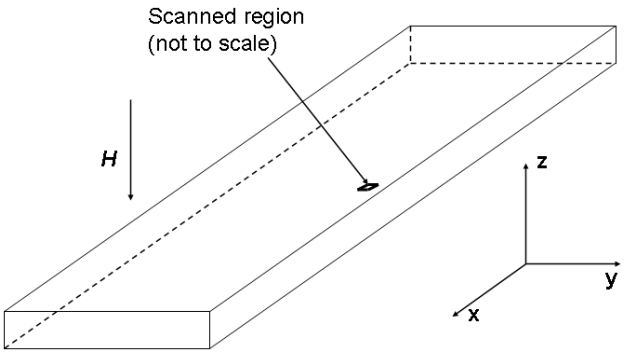

Figure 1. Sample and field geometry in our experiment.

probe microscopy. However, since the reported measurements were performed in zero-field-cooling conditions, one expects that upon increasing the external field, the field penetrates the film in flux bundles. The minimum detectable field in this experiment is $\sim$20 nTHz$^{-1/2}$. In the measurements presented here, the scan area is about 13 μm $\times$ 13 μm, divided into 128 $\times$ 128 pixels. Each local magnetic field B_{ij} (i, j = 1–128) is an average of 13 consecutive measurements.

The YBCO film was grown on an MgO substrate at 690 °C by electron beam co-evaporation of the metals in the presence of atomic oxygen with a subsequent anneal (also in atomic oxygen). The sample has a thickness of 350 nm, and a critical temperature of 86.4 K as measured by magnetization with a 10^3 A cm^{-2} persistent current density criterion, corresponding to the very foot of the resistive transition. For our studies, a piece 5 mm long and 2 mm wide was cut from a larger area film. In figure 1 is shown the geometry of our experiment.

3. Experimental results

After zero-field-cooling the sample at 80 K, we performed SHPM measurements at various applied magnetic fields, increasing from 0 to 31.7 Oe ($H_{\rm inc}$) and decreasing from 31 to 0 Oe ($H_{\rm dec}$). Each presented image is an average of 25 scans performed under the same conditions, and resulted in a map of the local magnetic induction, B_{ij}, as well as an average value of induction, $\langle B\rangle = \frac{1}{128\times128}\sum_{i,j=1}^{128} B_{ij}$, over the entire scan area and a greyscale (GS), $\delta B = \max(B_{ij}) - \min(B_{ij})$. We have observed that $\langle B\rangle$ does not depend significantly on the number of averages, while GS (and the image quality) increases with the number of averages and saturates (for this particular sample and Hall sensor) for 20–30 averages. Regarding the scale of imaging, it is obvious that both $\langle B\rangle$ and GS will depend both on the position of the scanned region in the film and on the dimensions of the scanned region. A (hypothetical) scan over the entire film surface would result in the same $\langle B\rangle$ as from a usual magnetization measurement using, for example, a SQUID magnetometer. Some of the resulting scans at 80 K are presented in figure 2 for increasing (figures 2(*a*)–(*d*)) and decreasing (figures 2(*e*)–(*i*)) applied fields.

Examining the images shown in figure 2 in more detail leads one to the following conclusions. In the earth field-cooled image (nominally $H_{\rm incr} \sim 0$ Oe), several vortices (white regions) can be distinguished, even if they are not clearly

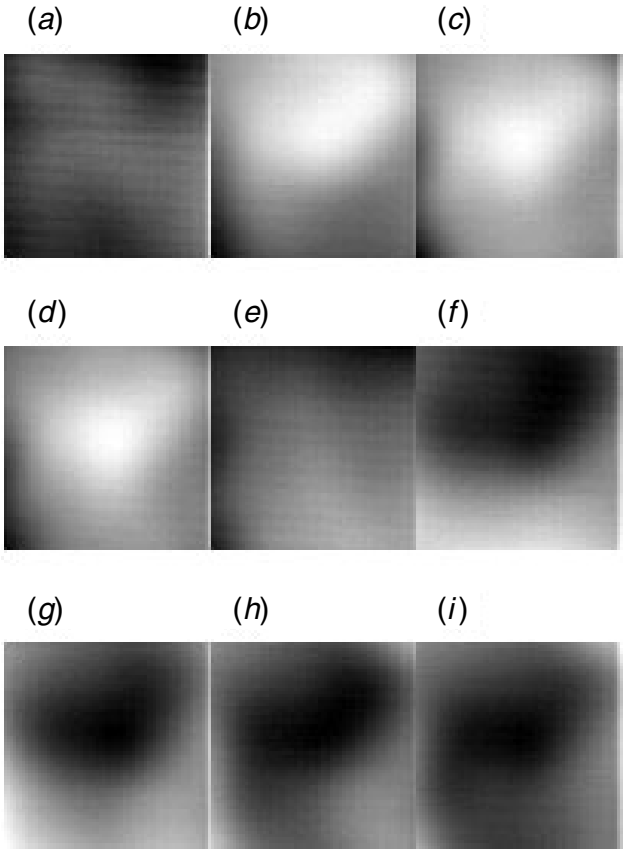

Figure 2. SHPM scans at several increasing and decreasing applied fields: (*a*) $H_{\rm inc} \sim 0$ (earth fieldcooled, $\langle B\rangle = 0.4$ G, greyscale (GS) ~ 0.93 G; (*b*) $H_{\rm inc} = 1$ Oe, $\langle B\rangle = 2.36$ G, GS ~ 2.1 G; (*c*) $H_{\rm inc} = 16$ Oe, $\langle B\rangle = 21.51$ G, GS ~ 2.1 G; (*d*) $H_{\rm inc} = 31.7$ Oe, $\langle B\rangle = 40.9$ G, GS ~ 2.2 G; (*e*) $H_{\rm dec} = 31$ Oe, $\langle B\rangle = 39.5$ G, GS $\sim$ 1.3 G; (*f*) $H_{\rm dec} = 30$ Oe, $\langle B\rangle = 36.7$ G, GS ~ 1.4 G; (*g*) $H_{\rm dec} =$ 28 Oe, $\langle B\rangle = 32.4$ G, GS ~ 1.8 G; (*h*) $H_{\rm dec} = 16$ Oe, $\langle B\rangle = 17.05$ G, GS ~ 1.2 G; (*i*) $H_{\rm dec} = 0$ Oe, $\langle B\rangle = -3.6$ G, GS ~ 1.2 G. Image size $\sim$13 μm $\times$ 13 μm.

separated. This implies, as expected, that the remanent field near the sample in our scanner head amounts to several tenths of an Oersted. At $H_{\rm inc} = 1$ Oe (figure 2(*b*)), additional flux enters the frame, mainly from the top right-hand corner, forming a large white flux bundle. Since the flux penetrated at such a small value of the applied field, and also $B > \mu_0 H$, it is evident that our scanned region is quite close to the edge of the film. A further increase in the applied field resulted in the increase of $\langle B\rangle$ and a slight re-positioning of the large vortex bundle towards the centre of the frame (figures 2(*c*) and (*d*)). After applying the maximum field of 31.7 Oe, just a small decrease of the field to 31 Oe led to the penetration of several vortices of opposite sign (antivortices) at the top right-hand corner of the frame, annihilating some of the vortices in the darker region there, as can be seen in figure 2(*e*). Even if there is a great difference in the images shown in figures 2(*d*) and (*e*), the corresponding values of $\langle B\rangle$ are not very different. Upon the applied field reversal, there seems to be a repositioning of some vortices and a partial annihilation of vortices by antivortices. The 'whitest' spot in figure 2(*e*) has a local field value of about $\langle B\rangle + \delta B/2 \cong 40.15$ G, while the 'darkest' spot has the corresponding value of

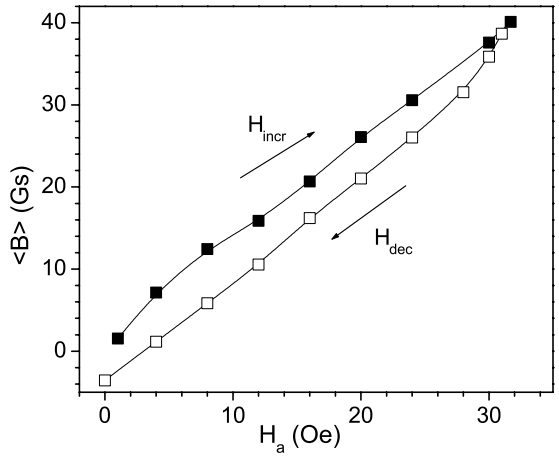

Figure 3. Applied field dependence of the average local magnetic induction ($\langle B\rangle$), for increasing and decreasing applied fields, as inferred from SHPM scans.

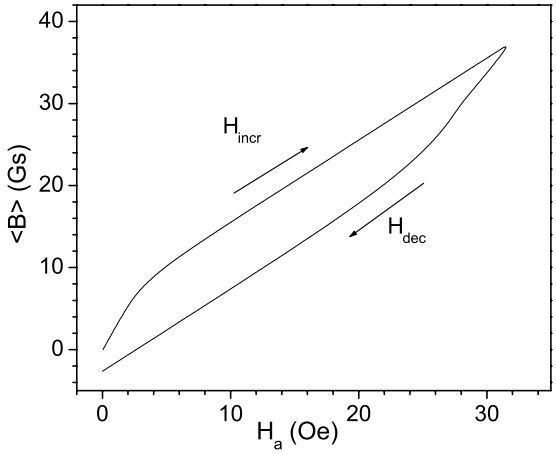

Figure 4. Numerical simulation of experimental data shown in figure 3, using equations (1) and (2), for $H_c = 4$ Oe and $y = 0.97$ mm.

$\langle B\rangle - \delta B/2 \cong 38.85$ G. At $H_{dec} = 30$ Oe (figure 2(f)), the dark region where vortices are partially annihilated by antivortices extends and becomes more pronounced, occupying the top of the frame. A further decrease in the applied field leads to small changes in the shape of the dark region and a slight repositioning of both its centre and the location of the darkest spot (figures 2(g) and (h)). In $H_{dec} = 0$ (figure 2(i)), the frame looks almost the same as for $H_{dec} = 16$ Oe (figure 2(h)), although the average field (remanent field) is now negative.

The dependence of the average magnetic induction $\langle B\rangle$ on the applied field is plotted in figure 3, showing some interesting features: (i) first of all (and most strikingly), we observe *inverse hysteresis*; $\langle B\rangle(H_{dec})$ smaller than $\langle B\rangle$ (H_{inc}) for the same value of H; (ii) secondly, we measure a *negative* remnant field once H_{dec} is returned to zero, as illustrated in scan figure 2(i). The very low field for vortex penetration, and the fact that $B > \mu_0 H_{inc}$ can be easily explained by the demagnetisation effects in our thin film geometry. The unusual features (i), (ii) will be addressed in the following discussion.

4. Discussion

Theoretical studies of flux penetration and profiles in thin, flat, superconductors with an applied field perpendicular to the sample plane were first reported by Brandt *et al* [3]. Since the general formulation [4], a large number of works have been devoted to the problem, in various geometries (strip, disk, square or arbitrary shape; finite or zero thickness) and using various approaches (critical state or more realistic current–voltage characteristics). Almost all of the studies provided *numerical* solutions arising from numerically-solved integrals. For the critical state approach, however, *analytic* solutions were derived for infinite-long strips [3], discs [5] and elliptic films [6] for the total magnetization of the sample.

For the conditions that apply in our measurements, however, analytic solutions were only derived, to the best of our knowledge, for the case of infinite-long flat strips. Briefly, the model [3] considers a flat superconducting strip with width $2a \gg d$ filling the space $|x| \leqslant d/2$, $|y| \leqslant a$, $|z| \leqslant \infty$, in which a spatially constant magnetic field H_a applied along x induces a supercurrent density $j(x, y)$ along z which is limited to a field-independent value j_c. The model does not distinguish Meissner surface currents and flux lines currents but considers only the smeared (over several flux line spacing) and integrated (over the thickness) current density $J(y)$. When H_a is increased from zero, the shielding current saturates near the specimen edges to $J(y > b) = J_c$ and $J(y < -b) = -J_c$ since flux starts to penetrate in form of flux lines such that $B(y) \neq 0$ for $|y| > b$ but still $B(y) \equiv 0$ for $-b < y < b$ ($b < a$), where $B(y)$ is the perpendicular component of magnetic field induction at the sample's surface and b is the position of the flux line front. The exact current distribution $J(y)$ of this two-dimensional problem with field-independent J_c was obtained by conformal mapping and the resulting $B(y)$, for $b < |y| < a$ (conditions that apply to our field-increasing experimental data), follows:

$$B = \mu_0 H_c \operatorname{arctanh}\{[y^2 - a^2/\cosh^2(H_a/H_c)]^{1/2}/|y| \times \tanh(H_a/H_c)\} \quad (1)$$

where $H_c = J_c/\pi$ is a critical field. After a maximum applied field H_0, it was shown that, for decreasing field from H_0 to H_a, the magnetic moment follows from the 'virgin' result by linear superposition of the form

$$B_{dec}(y, H_a, H_c) = B(y, H_0, H_c) - B(y, H_0 - H_a, 2H_c). \quad (2)$$

Using equations (1) and (2) several $B(y)$ dependencies are plotted in [3] at several applied fields, increasing from zero, as well as decreasing from H_0. The plots show that, very close to the film edge, i.e., $(a - y)/a \ll 1$, for increasing H_a the local magnetic induction $B > \mu_0 H_a$ and the remanent induction $B_{dec}(H_a = 0)$ can be negative, as in our measurements.

In our case, however, the distance y is a fixed parameter, and the variable is the applied field, while the situation is reversed in [3]. Equations (1) and (2) contain two effective fitting parameters, H_c and y, and our limited data set does not allow us to uniquely establish these. Our film has a rectangular shape, being about 5 mm in length, and $2a = 2$ mm in width and therefore is quite far from the 'infinite' long strip assumed in the theory. We are able to show, however, excellent agreement between theory and experiment for very reasonable choices for H_c and y. In figure 4, a simulation using equations (1) and (2)

is shown with $y = 0.97$ mm, and $H_c = 4$ Oe. Clearly, even if the assumptions of the model are not rigorously obeyed, the model provides an excellent qualitative description of our measurements, reproducing all the features discussed in part 3. Moreover, the simulation is quantitatively rather close to our data, although we note that other pairs of fitting parameters produce almost equally good agreement.

It is important to note that the observed negative remanent field and hysteresis inversion are *local phenomena* occurring only in flat (quasi-two-dimensional) superconductors in perpendicular geometry, and only near the edges of the sample, reflecting the strong demagnetizing effects and peculiarities of current and field profiles inside the sample in this geometry, in contrast to the original Bean model. Previous SHPM studies on similar films [7] with the scanning region far from the film edges did not show the unusual features reported here.

In conclusion, we have used SHPM to image vortex bundles and perform local magnetometry near the edge of a YBCO thin film. We obtain some rather unusual results, namely a very small field for vortex penetration, magnetization hysteresis inversion and a negative remanent magnetic induction. Our data are very well explained semi-quantitatively by a theoretical model of flux penetration in thin, infinitely-long strips.

Acknowledgment

This work was supported by EPSRC grant no GR/R46489/01.

References

[1] Bending S 1999 *Adv. Phys.* **48** 449
[2] Oral A, Bending S J and Henini M 1996 *Appl. Phys. Lett.* **69** 1324
[3] Brandt E H, Indenbom M V and Forkl A 1993 *Europhys. Lett.* **22** 735
[4] Brandt E H 1994 *Phys. Rev.* B **49** 9024
[5] Mikheenko P N and Kuzovlev Yu E 1993 *Physica* C **204** 229
[6] Mikitik G P and Brandt E H 1999 *Phys. Rev.* B **60** 592
[7] Grigorenko A N, Bending S J, Howells G D and Humphreys R G 2000 *Phys. Rev.* B **62** 721